

A Cellular Automaton Model of Excitable Media Including Curvature and Dispersion

MARTIN GERHARDT, HEIKE SCHUSTER, JOHN J. TYSON*

Excitable media are spatially distributed systems characterized by their ability to propagate signals undamped over long distances. Wave propagation in excitable media has been modeled extensively both by continuous partial differential equations and by discrete cellular automata. Cellular automata are desirable because of their intuitive appeal and efficient digital implementation, but until now they have not served as reliable models because they have lacked two essential properties of excitable media. First, traveling waves show dispersion, that is, the speed of wave propagation into a recovering region depends on the time elapsed since the preceding wave passed through that region. Second, wave speed depends on wave front curvature: curved waves travel with normal velocities noticeably different from the plane-wave velocity. These deficiencies of cellular automaton models are remedied by revising the classical rules of the excitation and recovery processes. The revised model shows curvature and dispersion effects comparable to those of continuous models, it predicts rotating spiral wave solutions in quantitative accord with the theory of continuous excitable media, and it is parameterized so that the spatial step size of the automaton can be adjusted for finer resolution of traveling waves.

PERIODIC TRAVELING WAVES IN EXCITABLE media provide dramatic illustrations of spontaneous spatiotemporal organization in biological, chemical, and physical systems. In biological contexts these propagating waves are used for communication, as in nerve axons and in neuromuscular tissue (1, 2). Similar waves of excitation are observed in homogeneous chemical systems (2, 3) and on catalytic surfaces (4). Wave propagation in these systems depends on a subtle interplay between the local dynamics of excitation and the diffusive coupling of neighboring spatial domains. The local dynamics of an excitable medium is characterized by a rest state that is stable with respect to small perturbations; however, when the system is perturbed beyond a certain threshold, it responds by going through a typical cycle of excitation and recovery to the rest state. A local region of excitation can then spread by diffusion to neighboring regions of resting (or recovering) medium.

Continuous partial differential equation (PDE) models of excitable media (2, 5-7) are often based on phase plane diagrams like that in Fig. 1a, which represents the local interactions between an excitation variable (u) and a recovery variable (v). Because the

excitation variable usually changes on a much faster time scale than the recovery variable, singular perturbation theory has been useful in analyzing wave propagation in such models (5-8). This theory highlights two important effects: dispersion and curvature. Dispersion refers to the dependence of wave speed on the extent of recovery of the

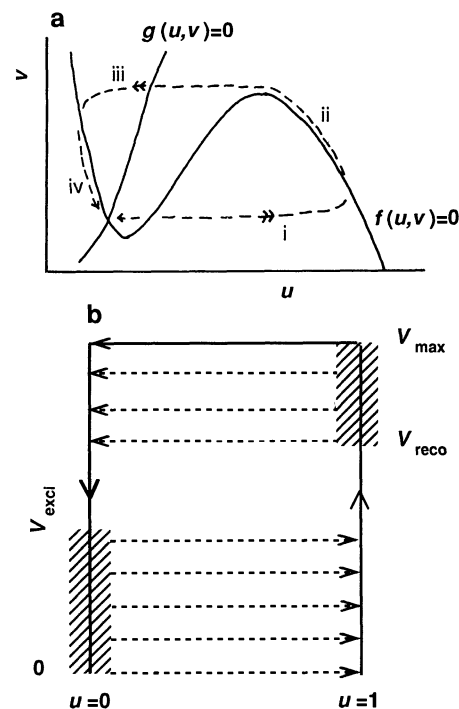
Fig. 1. (a) Typical phase plane diagram for an excitable medium. The excitation variable (u) and the recovery variable (v) interact locally according to the ordinary differential equations: $du/dt = f(u,v)$, $dv/dt = g(u,v)$. The loci $f(u,v) = 0$ and $g(u,v) = 0$, called "nullclines," are plotted in the (u,v) plane. There is a unique rest state at the intersection of the nullclines. The rest state is "excitable" in that small perturbations are immediately damped out, but larger perturbations (past threshold) trigger a long excursion during which (i) the excitation variable increases rapidly, causing (ii) a slower and temporary increase in v , followed by (iii) rapid extinction of u and (iv) slow decrease of v back to the rest state. For the Belousov-Zhabotinskii reaction, the excitation variable is bromous acid and the recovery variable is ferroin. For heart tissue, we can identify u with membrane potential and v with slow transmembrane ionic currents. **(b)** The local rules of the cellular automaton. The excitation variable u assumes two values: 0 [corresponding to the left-hand branch of the nullcline $f(u,v) = 0$] and 1 (the right-hand branch). The recovery variable v increases when $u = 1$ and decreases when $u = 0$. Waves of excitation (\rightarrow) can be triggered if the cell is sufficiently recovered (box on left), and waves of deexcitation (\leftarrow) can be triggered if the cell is sufficiently excited (box on right).

medium to the rest state. During periodic signaling (for instance, periodic firing of a sensory neuron in response to pressure), the excitable medium does not have enough time to recover completely to the rest state before the next wave is triggered. Consequently, the value of v at the moment of triggering is larger than the resting value of v (see Fig. 1a). At larger values of v , the medium is farther from threshold and requires greater excitation to trigger the next wave. To build up this extra excitation requires that the wave moves more slowly than a solitary wave propagating into fully recovered medium. This dependence of wave speed (c) on temporal period (T) is called the dispersion relation. In addition, the theory of traveling waves demonstrates that the curvature of wave fronts plays an essential role in the propagation of waves in two and three dimensions. Singular perturbation analysis of curved wave fronts leads to a relation between the normal velocity (N) and the curvature (K) of a propagating wave:

$$N = c + DK \quad (1)$$

where c is the speed of an uncurved (planar) wave front and D is the diffusion coefficient of the excitation variable. Equation 1 has been verified experimentally in a chemical excitable medium by Foerster *et al.* (9).

Rotating spiral waves are periodic patterns, and, far from the center of rotation, where the waves are nearly planar ($K \approx 0$), wave speed and period must satisfy the dispersion relation $c = F(T)$. Close to the pivot point where wave front curvature is



Department of Biology, Virginia Polytechnic Institute and State University, Blacksburg, VA 24061.

*To whom correspondence should be addressed.

appreciable, the curvature equation, Eq. 1, yields a second constraint between wave speed and period (5–7, 10), $T = G(c; r_0)$, which is parameterized by r_0 , a measure of the core size of the spiral. The intersection of the two curves, $c = F(T)$ and $T = G(c; r_0)$, determines the unique values of c and T for a spiral wave of core size r_0 . It is clear that, to understand the dynamics of rotating spiral waves in excitable media, we must have a realistic description of the effects of dispersion and curvature.

The theory of wave propagation in continuous models of excitable media does not obviate the need for numerical simulations. First of all, singular perturbation theory is an approximation tool, strictly valid only in the limit $\epsilon \rightarrow 0$ (where ϵ is the ratio of time scales for changes in the excitation and recovery variables). For real excitable media, with finite values of ϵ , we must check the results of the theory against numerical solutions of the underlying PDEs. Second, numerical simulations are an invaluable tool in exploring the complicated behavior of two- and three-dimensional excitable media. Indeed, most of the interesting behavior of these systems was found originally in numerical and experimental work, and the theoretical analysis came later. Because extensive numerical simulations of stiff (ϵ small) PDEs in two and three dimensions are difficult and costly (and were not even possible until recently), a different approach for exploring the temporal evolution of excitable media, based on discrete models, has played an important role.

The discrete approach was initiated in 1946 by Wiener and Rosenblueth (11), who were modeling rapid heart beat by high-frequency waves rotating around “obstacles” in a discrete model of excitable cardiac muscle. Later investigators demonstrated that rotating waves can persist even in unobstructed excitable media (12). In the discrete (“cellular automaton”) approach an excitable medium is represented by a grid of excitable elements that interact spatially with their nearest neighbors. Each element can exist in one of three states, resting, excited, or refractory, and these states may change in discrete time steps. A cell in the rest state will remain at rest unless one of its neighbors is excited, in which case the resting cell becomes excited in the next time step. Cells in the excited state become refractory, and refractory cells return to rest. Several elaborations of this basic idea have appeared (13, 14).

Cellular automaton models of excitable media have been popular for two reasons. First, they are intuitively appealing: compared to continuous models, they are easily

described and their behavior is easily comprehended. Second, they are easily implemented on digital computers, and, compared to numerical integration of PDEs, they run exceedingly fast. For the most part, cellular automaton models of excitable media have been kept quite simple, but in keeping to simplicity two critical features of wave propagation in excitable media, curvature and dispersion, have been left out. It is our intention to design a realistic cellular automaton model of excitable media that includes these effects.

We model an excitable medium by a rectilinear grid of cells, using no-flux boundary conditions. Each cell is characterized by internal state variables, and the state of a cell changes discretely in time depending on the state of the cell itself and the states of its neighbors. The dynamics of the cell itself should reflect the typical phase portrait of excitable media (Fig. 1a). Therefore, we introduce two state variables: an excitation variable (u) and a recovery variable (v). We assume that u takes only two values, 0 and 1,

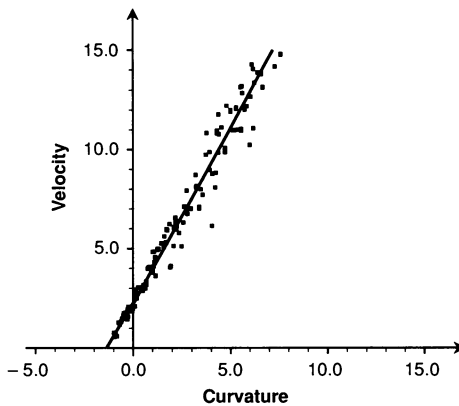


Fig. 2. Normal velocity as a function of curvature for concave and convex wave fronts. For this data set we took $r = 3$ and $k_{\text{exci}}^0 = 8$. The other parameter values are irrelevant to the curvature effect.

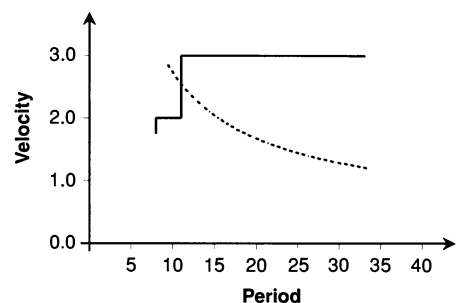


Fig. 3. The dispersion and curvature relations for the cellular automaton. The dispersion relation (solid line) was calculated for the parameter values: $V_{\text{max}} = 100$, $V_{\text{reco}} = 90$, $V_{\text{exci}} = 85$, $g_{\text{up}} = 25$, $g_{\text{down}} = 20$, $k_{\text{exci}}^0 = 5$, $k_{\text{reco}}^0 = 7$. The curvature relation (dashed line) was calculated from the approximate analytical equation in (10) for $r_0 = 2.5$ and $D = 1.6$.

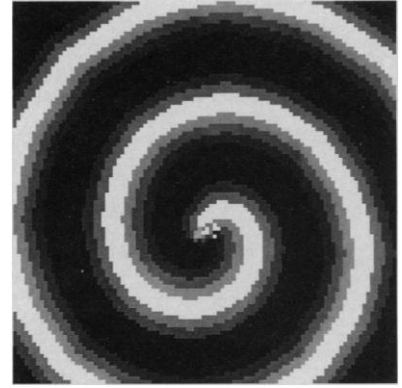


Fig. 4. Spiral wave solution of the cellular automaton for the parameter values given in Fig. 3. The size of the field is 100 by 100. This solution was initiated by a “broken” wave front that extended from the right boundary to the middle of the domain.

whereas v takes integer values $0, 1, 2, \dots, V_{\text{max}}$. The state $u = 0, v = 0$ is the rest state. If $u = 1$, the cell is in an “excited” state, and if $u = 0, v \neq 0$, the cell is in a “recovering” state. In an excited state v should increase from time step t to $t + 1$, and in a recovering state v should decrease. Therefore, we specify that

$$\text{If } u_t = 1, \text{ then } v_{t+1} = \min\{v_t + g_{\text{up}}, V_{\text{max}}\} \quad (2)$$

and

$$\text{If } u_t = 0, \text{ then } v_{t+1} = \max\{v_t - g_{\text{down}}, 0\} \quad (3)$$

where g_{up} and g_{down} are positive integers. (We choose linear kinetics for simplicity.) In the absence of interactions with neighbors, the local rules should permit a cell to jump autonomously from the excited state to the recovering state when v reaches V_{max} but not from the recovering state to the excited state. We express this as follows:

$$\text{If } u_t = 0, \text{ then } u_{t+1} = 0 \quad (4)$$

$$\text{If } u_t = 1, v_t \neq V_{\text{max}}, \text{ then } u_{t+1} = 1 \quad (5)$$

$$\text{If } u_t = 1, v_t = V_{\text{max}}, \text{ then } u_{t+1} = 0 \quad (6)$$

These local rules specify a discrete version of the typical phase portrait of excitable media (Fig. 1b).

A resting or recovering cell can become excited only by interaction with its neighbors. We assume that a cell becomes excited if and only if the number of excited cells within its neighborhood exceeds a certain threshold, k_{exci} (k_{exci} reflects the “excitability” of the medium: smaller values of k_{exci} represent higher excitabilities). Furthermore, a cell can become excited only if it is sufficiently recovered, that is, $0 \leq v_t < V_{\text{exci}} < V_{\text{max}}$. In this way we divide recovering cells into two categories: absolutely refractory ($V_{\text{exci}} \leq v \leq V_{\text{max}}$) and relatively

refractory ($0 < \nu < V_{\text{exci}}$). Similarly, we propose that an excited cell can jump “prematurely” to the recovering state if it is neighbored by a sufficient number of resting and recovering cells (k_{reco}), and if $0 < V_{\text{reco}} < \nu_t < V_{\text{max}}$. In the context of excitable media, we insist that $V_{\text{exci}} < V_{\text{reco}}$.

To ensure that the excitability of the medium depends on its extent of recovery, we assume that k_{exci} is an increasing function of ν on the interval $0 \leq \nu \leq V_{\text{exci}}$. That is, for a relatively refractory cell to become excited, we require a greater amount of excitation in its neighborhood. Similarly, we make k_{reco} a decreasing function of ν on the interval $V_{\text{reco}} \leq \nu \leq V_{\text{max}}$ (15).

The neighborhood of a cell is taken to be the square of edge-length $2r + 1$ ($r = 1, 2, 3 \dots$) centered on the cell (16). We call r the radius of the neighborhood. Larger neighborhoods give finer spatial resolution to our automaton: as r increases, we increase the number of grid points per unit length (the length over which spatial interactions are effective in one time step). For instance, large values of r allow a range of propagation velocities of planar waves, which is clearly necessary to model the effects of dispersion.

The effects of curvature on wave propagation in excitable media are seen most dramatically when waves from two different sources collide (9). We simulated wave collisions with our automaton, fitting each successive position of the wave front with hyperbolas in the regions of largest positive and negative curvature. From the best fitting hyperbolas we calculated normal velocities (N) and curvatures (K). These data were then fitted by a straight line, as suggested by Eq. 1. A typical result is illustrated in Fig. 2.

For all parameter values the dependence of N on K is linear, verifying that our automaton satisfies Eq. 1. The slope of the line (D , the diffusion coefficient of the excitation variable) depends on the radius r and increases in direct proportion to the area of the neighborhood, $D(r) \cong 0.032(2r + 1)^2$, exactly what would be expected of a diffusion coefficient as the spatial grid is made finer. If we equate $D(r)$ to the measured diffusion coefficient of the excitation variable of a particular excitable medium, we have one equation connecting the time and space scales of the automaton. We obtain a second relation between these two unknowns by equating the speed of a solitary planar wave in the automaton to the measured speed of such a wave in the excitable medium. In this way we can associate absolute values to the time step and spacing of cells in our automaton (17).

To calculate dispersion relations, c versus T , we simulated our automaton on a ring-shaped domain. We initiated a pulse traveling in one direction around the ring. After transients had died out, we measured the period of circulation of the pulse. From the period T and wavelength λ (circumference of ring), we calculated the average speed $c = \lambda/T$. A representative result is presented in Fig. 3.

For these same parameter values, the unique spiral wave solution of the cellular automaton is illustrated in Fig. 4. The spiral rotates with a period of 11 time steps and has an asymptotic wave speed of 2.5 cells per time step (18). According to singular perturbation theory (5, 6), the wave speed and period of spiral wave solutions to reaction-diffusion equations should satisfy simultaneously both the dispersion relation, $c = F(T)$, and the curvature relation, $T = G(c; r_0)$. For the cellular automaton model, the calculated spiral wave is consistent with the dispersion relation and the curvature relation for core size $r_0 = 2.5$ (Fig. 3). To be completely consistent, this predicted value of r_0 should agree with observations of the core of the spiral wave in Fig. 4. It is not easy to determine from the computations the radius r_0 required by theory, but a slightly smaller radius r_q can be estimated as

follows. At each time step we determine the position of the “phase change” (7) point, q , which lies at the junction of the wave front (cells where ν switches from 0 to 1) and the wave back (from 1 to 0). During one rotation the phase change point traces a path surrounding an area that we equate to πr_q^2 . In this fashion we measure $r_q = 2.2$ for the spiral wave in Fig. 4, a value that is in excellent agreement with the expected value of r_0 .

The spiral depicted in Fig. 4 rotates more or less rigidly around a pivot point, but for other parameter values we have observed (i) meandering spiral cores (19) and (ii) chaotic self-reproduction of spirals by spontaneous wave-breaking (1, 20) (Fig. 5). The spontaneous multiplication of spiral wave cores in an excitable medium may have relevance to the onset of ventricular fibrillation. Ventricular flutter (“tachycardia” or rapid heart beat) is widely attributed to the generation of a high-frequency rotating spiral wave in the ventricular myocardium (2, 12, 21). Although ventricular flutter is not in itself life-threatening, it may degenerate into fatal fibrillation (a chaotic disorganized rapid convulsion of the ventricle) by the spontaneous breakup of the original spiral wave (or pair of counterrotating spirals) into myriad spiral sources distributed throughout the

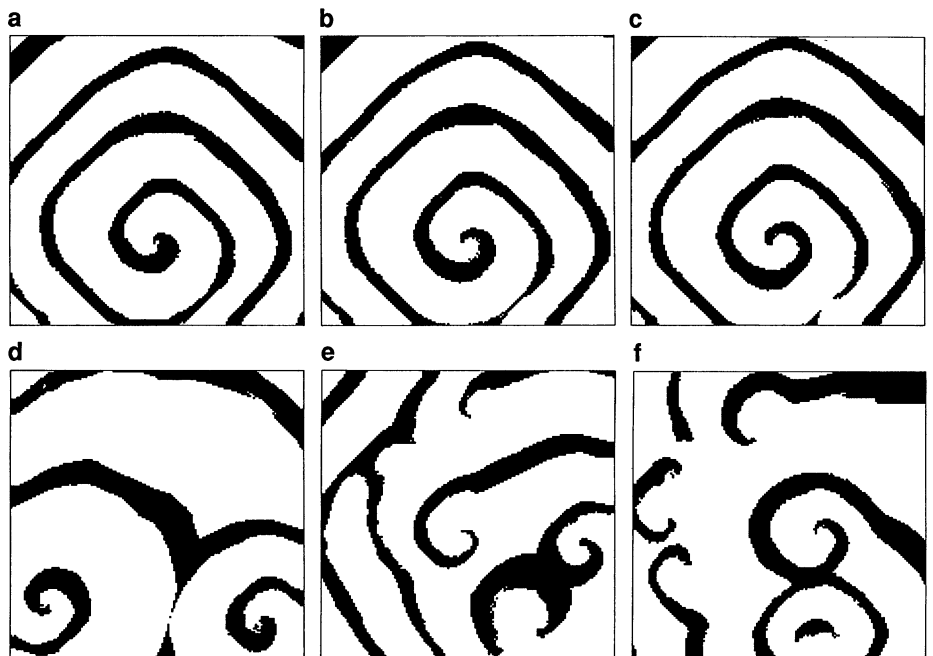


Fig. 5. Chaotic self-reproduction of spiral waves. (Parameter values: grid = 150 by 150, $r = 3$, $V_{\text{max}} = 100$, $V_{\text{reco}} = 70$, $V_{\text{exci}} = 65$, $g_{\text{up}} = 20$, $g_{\text{down}} = 5$, $k_{\text{exci}}^0 = 0$, $k_{\text{reco}}^0 = 5$.) The original spiral wave is breaking near the lower edge of the domain, (a) $t = 155$, (b) $t = 157$, (c) $t = 159$. The breakup generates a pair of counterrotating spiral waves in addition to the original rotor. One member of the counterrotating pair is absorbed by the boundary shortly after its creation, leaving two spirals of the same sense of rotation, (d) $t = 319$. Next, the original spiral disappears, but the remaining rotor multiplies itself by spontaneous wave-breaking until there are many rotors in the domain, (e) $t = 584$. The process of birth, meandering, and death of rotors continues, (f) $t = 667$, so that the pattern is ever-changing in an unpredictable fashion. The fundamental period of the process, determined by Fourier analysis, is 25 time steps.

ventricle. The breakup process is not thoroughly understood, but it is usually attributed to spatial inhomogeneities of the cardiac muscle (13), for instance, local regions of inexcitability caused by coronary artery disease. Our cellular automaton model (Fig. 5) suggests that the breakup of a spiral wave may occur in a spatially homogeneous medium by spontaneous processes implicit in the mechanism of excitability. Close examination of the calculations reveals that the breakup of excitation waves occurs because the wave front is slowed down by momentary refractoriness of the recovering medium ahead of the wave, but the wave back continues propagating at a greater speed than the wave front. The wave back catches up to the wave front and annihilates it (Fig. 5, a through c) (22). There follows a complicated sequence of spiral wave creation and destruction, generating complicated transient patterns (Fig. 5, d through f), until at $t = 9479$ all spontaneous excitation ceases. Since for heart tissue one time step ≈ 3 ms (17), the entire "fibrillation" episode has lasted about 30 s.

Our cellular automaton model is based firmly on the properties of excitation and recovery that are essential to excitable media. It incorporates, in quantitative detail, the effects of curvature and dispersion on wave propagation, in particular, on the speed and period of rotating spiral waves. By increasing the radius of the neighborhood one can control the spatial resolution of the automaton in much the same way that step sizes can be adjusted in the numerical solution of PDE models. Nonetheless, the cellular automaton is still orders of magnitude faster than comparable numerical solution of PDEs (23). We intend to exploit the fidelity and speed of our model in simulations of scroll wave evolution in three-dimensional excitable media.

REFERENCES AND NOTES

1. A. T. Winfree, *J. Theor. Biol.* **138**, 353 (1989).
2. ———, *When Time Breaks Down* (Princeton Univ. Press, Princeton, NJ, 1987).
3. R. J. Field and M. Burger, Eds., *Oscillations and Traveling Waves in Chemical Systems* (Wiley, New York, 1985).
4. J. R. Brown, G. A. D'Netto, R. A. Schmitz, in *Temporal Order*, L. Rensing and N. I. Jaeger, Eds. (Springer-Verlag, Berlin, 1985), pp. 86–95; M. Gerhardt and H. Schuster, *Physica D* **36**, 209 (1989).
5. J. P. Keener, *Soc. Ind. Appl. Math. J. Appl. Math.* **46**, 1039 (1986); ——— and J. J. Tyson, *Physica D* **21**, 307 (1986).
6. J. J. Tyson and J. P. Keener, *ibid.* **32**, 327 (1988).
7. V. S. Zykov, *Simulation of Wave Processes in Excitable Media* (Manchester Univ. Press, Manchester, United Kingdom, 1987).
8. ———, *Biophysics (USSR)* **25**, 329 (1980); *ibid.*, p. 906; P. C. Fife, in *Non-Equilibrium Dynamics in Chemical Systems*, C. Vidal and A. Pacault, Eds. (Springer-Verlag, Berlin, 1984), pp. 76–88; J. J. Tyson, *J. Chim. Phys. Phys. Chim. Biol.* **84**, 1359 (1987).
9. P. Foerster, S. C. Müller, B. Hess, *Science* **241**, 685 (1988); *Proc. Natl. Acad. Sci. U.S.A.* **86**, 6831 (1989).
10. The curvature constraint, derived by Tyson and Keener (6), is a relation between asymptotic wave speed (c), temporal period (T), and core size (r_0): $D/Tc^2 = 8\pi [1 + (D/r_0)]/[1 + (4c\sigma_0/D) - \sqrt{1 + (8c\sigma_0/D)}]$.
11. N. Wiener and A. Rosenbluth, *Arch. Inst. Cardiol. Mex.* **16**, 205 (1946).
12. B. G. Farley, *Comput. Biomed. Res.* **1**, 265 (1965); I. S. Balakhovsky, *Biophysics (USSR)* **10**, 1175 (1965).
13. G. K. Moe and J. A. Abildskov, *Am. Heart J.* **58**, 59 (1959); G. K. Moe, W. C. Rheinboldt, J. A. Abildskov, *ibid.* **67**, 200 (1964); V. I. Krinsky, *Biophysics (USSR)* **11**, 776 (1966); J. M. Smith and R. J. Cohen, *Proc. Natl. Acad. Sci. U.S.A.* **81**, 233 (1984).
14. J. M. Greenberg and S. P. Hastings, *Soc. Ind. Appl. Math. J. Appl. Math.* **34**, 515 (1978); J. M. Greenberg, B. D. Hassard, S. P. Hastings, *Bull. Am. Math. Soc.* **84**, 1296 (1978); V. S. Zykov and A. S. Mikhailov, *Sov. Phys. Dokl.* **31**, 51 (1986); M. Markus and B. Hess, in *Dissipative Structures in Transport Processes and Combustion*, D. Meinköhn, Ed. (Springer-Verlag, Berlin, in press). Markus and Hess have incorporated curvature effects into their automaton by introducing a randomized spatial grid.
15. We assume linear dependencies of k_{exci} and k_{reco} on v : $k_{\text{exci}}(v) = k_{\text{exci}}^0 + [r(2r+1) - k_{\text{exci}}^0](v/V_{\text{exci}})$, and $k_{\text{reco}}(v) = k_{\text{reco}}^0 + [r(2r+1) - k_{\text{reco}}^0][(v - V_{\text{max}})/(V_{\text{reco}} - V_{\text{max}})]$.
16. The spatial domain is uniform and isotropic by assumption. An anisotropic medium could be modeled with a rectangular neighborhood.
17. For the Belousov-Zhabotinskii reaction, the diffusion coefficient for bromous acid is 2×10^{-3} mm²/s and the speed of a planar solitary wave is 0.1 mm/s, so one cell in our automaton (with $r = 3$) corresponds to 0.03 mm and one time step ≈ 1 s. For heart tissue, the effective diffusion coefficient for membrane potential is 0.6 cm²/s and the speed of planar solitary waves is roughly 30 cm/s, so with $r = 3$, one cell ≈ 0.3 mm and one time step ≈ 3 ms.
18. Using the space and time scales estimated for the Belousov-Zhabotinskii reaction in (17), we find that the spiral wave in Fig. 4 has a period of 11 s, a wave speed of 75 μ m/s, and a wavelength of 0.8 mm. These values are comparable to the data observed for spirals in the Belousov-Zhabotinskii reaction, for example, S. C. Müller, T. Plessner, B. Hess, *Science* **230**, 661 (1985).
19. O. E. Rössler and C. Kahlert, *Z. Naturforsch. Teil A* **34**, 565 (1979); W. Jahnke, W. E. Skaggs, A. T. Winfree, *J. Phys. Chem.* **93**, 740 (1989).
20. Y. Kuramoto and S. Koga, *Prog. Theor. Phys.* **66**, 1081 (1981); A. T. Winfree, in *Cardiac Electrophysiology, from Cell to Bedside*, D. P. Zipes and J. Jalife, Eds. (Saunders, Philadelphia, in press).
21. M. A. Allesie, F. I. M. Bonke, F. J. G. Schopman, *Circ. Res.* **33**, 54 (1973); E. Downar et al., *J. Am. Coll. Cardiol.* **4** (no. 4), 703 (1984); N. Shibata et al., *Am. J. Physiol.* **255**, 891 (1988); D. W. Frazier et al., *J. Clin. Invest.* **83**, 1039 (1989).
22. This annihilation process is not necessarily an artifact of the discrete nature of our cellular automaton, because spontaneous annihilation of excitation waves has been observed in the Belousov-Zhabotinskii reaction [M. L. Smoes, in *Dynamics of Synergetic Systems*, H. Haken, Ed. (Springer-Verlag, Berlin, 1980), pp. 80–96] and in computations on models of heart tissue (J. P. Keener, personal communication).
23. One revolution of the spiral wave in Fig. 4 takes 2 s of central processing unit (cpu) time on a VAXstation 3200. A comparable calculation of one revolution of a spiral wave in a PDE model of the Belousov-Zhabotinskii reaction requires about 40 min of cpu time on the same computer. Most of the acceleration can be attributed to the fact that, because of the rapid changes registered by the excitation variable, the PDE integration routine must take temporal steps 150 times shorter than the size of the temporal step of the cellular automaton.
24. This work was supported by the National Science Foundation, grant DMS-8810456 (to J.J.T.), and by the Deutsche Forschungsgemeinschaft (to H.S.). The State Council of Higher Education in Virginia purchased the VAXstation 3200, on which all calculations were carried out. We acknowledge helpful discussion over several years with J. P. Keener, A. T. Winfree, G. B. Ermentrout, and A. Dress.

16 October 1989; accepted 18 January 1990